



HUNGARIAN UNIVERSITY OF AGRICULTURE AND LIFE
SCIENCES

Pre-treated pine waste as an alternative energy
source

PhD thesis

by

Alok Dhaundiyal

Gödöllő
2021

Doctoral school

denomination: Doctoral School of Mechanical Engineering

Science: Mechanical Engineering

Leader: Prof. Dr. Farkas István, DSc
Institute of Technology
Hungarian University of Agriculture and Life Sciences,
Godollo, Hungary

Supervisor: Prof. Dr. Laszlo Toth, DSc
Institute of Technology
Hungarian University of Agriculture and Life Sciences,
Gödöllő, Hungary

Dr. Nobert Schrempf, PhD
Institute of Technology
Hungarian University of Agriculture and Life Sciences,
Gödöllő, Hungary

.....

Affirmation of head of school

.....

Affirmation of supervisor

CONTENTS

LIST OF SYMBOLS AND ABBREVIATIONS.....	4
1. INTRODUCTION, OBJECTIVES	5
1.1. Introduction	5
1.2. Objectives	5
2. MATERIALS AND METHODS	6
2.1. Fuel preparation and densification by pelletising	6
2.2. Improvisation of a Joule heating system	7
2.3. Construction detail of a packed-bed reactor	8
3. RESULTS AND DISCUSSION	10
3.1. Structural evaluation of pine needles	10
3.2 Structural evaluation of pine cones	10
3.3. Thermal performance of pine needles in a small-scale reactor	11
3.4. Thermal performance of pine cones in a small-scale reactor	14
3.5. Heat of reaction for pine needles	18
3.6. Heat of reaction for pine cones	19
4. NEW SCIENTIFIC RESULTS	21
5. CONCLUSION AND SUGGESTIONS	24
6. SUMMARY..	25
7. MOST IMPORTANT PUBLICATIONS RELATED TO THE THESIS	26

LIST OF SYMBOLS AND ABBREVIATIONS

T	Temperature	$^{\circ}\text{C}$
ΔP	Pressure drop	Pa
FCR	Fuel consumption rate	$\text{kg}\cdot\text{s}^{-1}$
SPR	Specific pyrolysis rate	$\text{kg}\cdot\text{s}^{-1}\cdot\text{m}^{-2}$
$SGPR$	Specific gas production rate	$\text{m}\cdot\text{h}^{-1}$
ε	Void fraction of packed bed	-
μ	Dynamic viscosity of gas	$\text{N}\cdot\text{s}\cdot\text{m}^{-2}$
ψ	Sphericity of a pellet	-
g	Subscript represents gas	-
f	Subscript denotes solid fuel	-
p_v	The partial pressure of water vapour	Pa
p_s	Saturated pressure of water vapour	Pa
b	Subscript denotes the bed	-
c	Subscript represents cold gas	-
h	Subscript denotes hot gas	-
t	Subscript stand for thermal efficiency	-
η	The efficiency of a reactor	-
S_s	The surface area of a spherical pellet	m^2
S_p	The surface area of a pellet	m^2
ω	Specific humidity	$\text{kg}(\text{w.v.})\cdot\text{kg}(\text{d.g.})^{-1}$
γ	Degree of saturation	-
τ	Time required to consume biomass	h
\bar{h}	The average value of the heat transfer coefficient	$\text{W}\cdot\text{m}^{-2}\cdot\text{K}^{-1}$
p	Pressure exerted by producer gas	Pa
$Ac.s$	Cross-sectional area of a reactor	m^2
H	Height of a reactor	m
ΔH	Heat of reaction	$\text{kJ}\cdot\text{kg}^{-1}$
DTA	Differential thermal analysis	
DTG	Derivative thermogravimetry	
FESEM	Field emission scanning electron microscopy	
TCD	Thermal conductivity detector	
HBM	Hottinger Baldwin Messtechnik	

1. INTRODUCTION, OBJECTIVES

The significance, novelty, and objectives of the research work have been discussed in this chapter.

1.1. Introduction

By definition, biomass refers to how much tissue mass for a population is available at a particular instant of time or averaged over several periods. It is often reported either in the context of mass (g) or energy (J) per unit area. The broader perspective includes the organic matter of plants (under and above the ground), but it is not limited. The organic matter in the soil does not fall in the biomass domain, yet some of them come under the purview of it: bacteria, fungi and meiofauna. However, soil biomass covers less than 5% of soil organic matter.

The novelty of research work

A prevailing methodology for thermal pre-treatment of the material focuses on the application of micro-waves, which pivoted around varying power output and varying operating frequency. The ramification of micro-wave torrefaction leads to cold spots within the material and poor texture due to intermolecular friction. Apart from the material properties, the risk of contamination and leakage of radiation poses a serious health hazard. Some studies have also been carried out on the modified version of the micro-wave system.

1.2. Objectives

The research work encompasses the detailed analysis of the thermal pre-treatment process and its effect on the physical, chemical and structural characterisation of the waste materials. The quasi-static technique was adopted whilst performing torrefaction in the modified Joule heating system, and based on the factors mentioned above, the objectives of this research are elucidated as follow:

- The effect of the operating condition on physicochemical traits of the processed substrate obtained by the new methodology.
- The change in the morphology of raw pine waste upon varying thermodynamic state of pine waste.
- Thermal performance of the torrefied material in a packed-bed pyrolysis reactor.
- Energy economics of the derived material after the quasi-static torrefaction.

2. MATERIALS AND METHODS

The material and methods are classified according to the operation conducted upon the waste material derived from black pine. The techniques used to analyse the samples of material are also covered under this heading. The sophisticated measurements were performed in the Indian Institute of Technology, Roorkee, Uttarakhand, India, whereas some physical analyses were partly carried out in the National Agriculture and Innovation Centre, Hungary and the Energy Laboratory of Institute of Process Engineering, Szent Istvan University, Hungary.

2.1. Fuel preparation and densification by pelletising

The net 10 kg of pine waste (pine needles and pine cones) was collected from the Pest county of Hungary. After collecting the raw material, it was sundried for a week in a sieved frame. The collected material is illustrated in Fig.1. For the milling purpose, a 3-phase heavy-duty 1.5 kW rotor milling machine (6-disc rotor) (Retsch SM 2000) was considered. The material was fed tangentially through a standard hooper (80mm ×80 mm). For a given material, the feeding rate was kept between 200 to 300 g·h⁻¹. The material experienced a plastic deformation through a sieve size of 1.5 mm. The net material collected at the end of the milling process with an average processing efficiency of 70% was 7 kg. After milling the feedstock, the moisture content was measured. It is to be noted that 1–2% of water is supplied to the milled form of material, which is thereby heated to approximately 70 °C. The heat ensures that the lignin in the wood is released and it would contribute to increasing the binding of the particles in the end-product.



Fig. 1. The collected pine waste (pine needles and pine cone)

The densification of the prepared pine waste was performed using a ring-type pellet machine (CL3, Pellet mill). A screw extrusion of prepared feedstock was initiated by feeding the fine powder into a barrel through a long material hooper (feeding capacity of 0.014 m^3). The objective of the screw is to push the material into the chamber where a roller presses the material radially outward through the cylindrical grooves provided on the circumference of the ring die. The estimated length and diameter was calculated to be 25.95 mm and 6.39 mm, respectively. The processed pellet is shown in Fig. 2.



Fig. 2. The pelletised form of pine waste for dust removal

2.2. Improvisation of a Joule heating system

The torrefaction process was performed under a pilot scheme. A digitally programmed furnace (Nabertherm GmbH) based on the Joule heating was modified to carry out the thermal pre-treatment in the quasi-static condition. The furnace used during the testing process is illustrated in Fig. 3 (a). The technical drawing of the furnace is provided in Fig. 3 (b). For scavenge process, the nitrogen gas was allowed to flow with a volumetric rate of $42 \text{ L}\cdot\text{min}^{-1}$. The flow of nitrogen deters the diffusion of the present oxygen and prevent the surface oxidation reaction at the surface of the material. The mass measurement was performed by connecting the mass holder to the weighing machine via a mechanical link. The lid ($313.15 \text{ mm} \times 250 \text{ mm}$) for the furnace was fabricated in such a manner that could hold the pine pellets without heating them. A hollow cylinder having a length of 559.8 mm along with a ramrod was provided with the lid for carrying the material unless the furnace attains the desired temperature. To hold the lid with the furnace, a steel bracket was used. Apart from the cylindrical accoutrement, the nitrogen ducts of 21.5 mm each in diameter were carved out on the hollow cylinder and the rectangular frame of the lid. To cool down the system, a fan was bolted along the structure to inhibit the heating of protruded cylindrical section. The pre-treated pellet is shown in Fig. 4.

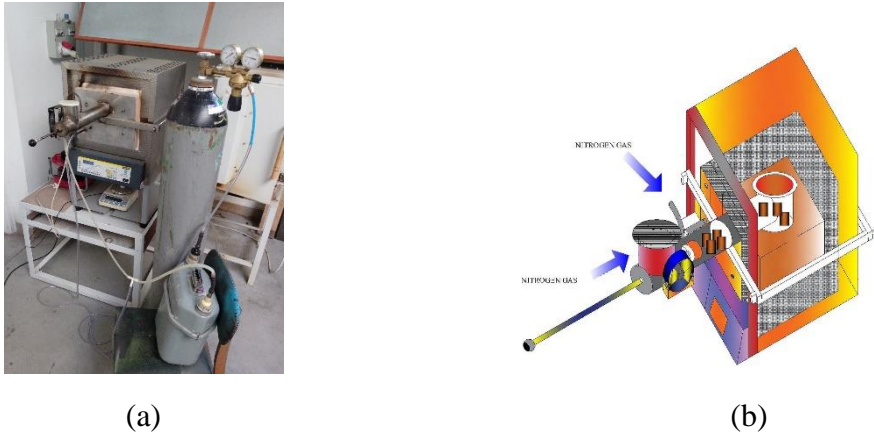


Fig. 3. Torrefaction unit for pre-treatment of pine waste (a– Improvised Joule heating system, b– Technical drawing of heating system)



Fig. 4. The upgraded pine waste after thermal pre-treatment

2.3. Construction detail of a packed-bed reactor

The preliminary drafting of the reactor was executed in AutoCAD (Autodesk, 2019). The inner shell of the reactor was fabricated from 1.45 mm thick welded carbon steel. The height of the reactor from the base was decided to be 430 mm, whereas the inner length was estimated to be 400 mm. A clearance of 30 mm was provided between the inner shell and the outer shell. The rock wool having a thickness of 41.5mm was coated around the inner shell to fend off the heat loss across the outer shell of the reactor. The material used for manufacturing the outer shell was a galvanised steel sheet. The diameter of the outer and inner shells of the reactor was estimated to be 165 and 85.2 mm, respectively. The technical sketch of the reactor is provided in Fig. 5 (a), whereas the physical form of the reactor is shown in Fig. 6 (b). The six measurement ports for thermocouples were etched along the diametrical axis of the shells. However, the four measurement ports (A, B, C and D) were only used during the measurement process (Fig. 5(a)).

2. Materials and methods

The distance between ports was made to be 43.8 mm. For pressure measurement, a small duct of diameter 5 mm was welded on the top stainless-steel cover plate. The pressure sensor used for measurement was a current-based transducer (Huba Control).

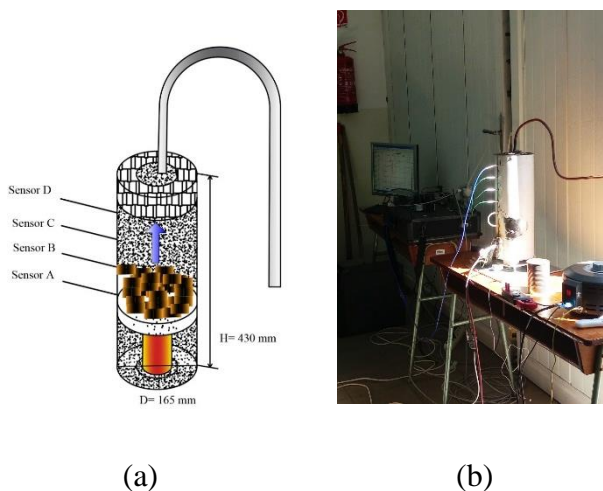


Fig. 5. A fixed bed pyrolysis reactor (a: Technical drawing of pyrolysis reactor, b: The reactor retrofitted with the ancillary components)

The measurement of thermodynamic properties of the system was done by a 16-channel data acquisition unit (HBM). The thermogravimetric evaluation was carried out by a strain gauge (HBM) (voltage type, full-bridge Wheatstone, type II). To calibrate the strain gauge, a 500 g of iron weight was taken to determine the accuracy and precision of the mass measurement system. The thermocouples type K (Ni-Cr) were used to determine the temperature at the designated ports (A, B, C and D) provided along the circumference of the outer shell of the reactor. The producer gas measurement and its sampling were performed with the help of the wood gas analyser (VISIT-03 H, Messtechnik EHEIM GmbH). The sampling rate was preset at a volumetric rate of $0.7 \text{ L}\cdot\text{min}^{-1}$.

The gas analyser not only determines the % fraction of producer gas but also provides the gas wash to cool the hot gas. The gash wash bottles filled with refined oil and the distilled water were used to trap the gaseous by-products formed during pyrolysis reactions. Once the gas got cleaned, it went for further processing in the wool filter, activated carbon, and activated alumina soaked in potassium permanganate so that the dry producer gas could be obtained.

3. RESULTS AND DISCUSSION

The study is divided among physical and chemical characteristics of thermally pre-treated, topological changes induced due to torrefaction, and the effect of torrefaction on thermodynamics and chemical kinetics. The pine waste comprises pine needles and pine cones, whereas the results are compared and validated with the experimental studies conducted in non-isothermal conditions.

3.1. Structural evaluation of pine needles

The topological changes upon thermal pre-treatment were studied with the help of FESEM. It was found that the bigger cleavage on the surface of pine needles propagated along the surface at an orientation between 13–30°, whereas the small cracks on the cellulose fibre were noticed to incline 108–121°. The length of macro cracks formed during torrefaction varied from 8.08 μm to 20.77 μm , whereas the width was estimated to be in the range of 11.41–204.33 μm . On the other hand, the length of small cracks on the cellulose fibre falls in the domain of 4.503–30.32 μm . The effective width of small fissures was determined in the range of 1.32–3.29 μm . The recorded area of small fissures was computed to be 72% less than that of big cracks. The microfibrils were completely decomposed into small splinters. The cellulose structure was noticed to be devoid of amorphous segments. The macropores were noticed to be dilated in the interval of 2.82–9.65 μm . The orientation of macropores was stretched from 17° to 123°. The area of micro fibrillated cellulose was evaluated to be 2.77 μm^2 , whereas its diameter was found to vary in the range of 9.66–33.64 μm . The surface area of cellulose fibre was slightly increased due to the thermal pre-treatment.

3.2 Structural evaluation of pine cones

Likewise, pine needles structure, the microfibrils of raw pine cones was dilated by 198.5% after thermal pre-treatment. The diameter of the microfibril was estimated to lie in the domain of 27.72–68.88 μm . The big cracks of mean length 65.49 μm were found at the corners of cellulose fibre. A small fissure of 1.47–10.43 μm was noticed between the grain boundaries of pine cones. The orientation of the grain was deviated by 28–47° after the pre-treatment. The wall of native cellulose fibre was remained intact and there were no structural defects found. The cellulose fibre of thermally processed pine cones was stretched by 13%, whereas the surface area of fibre was increased by 12%. Similar to pine needles, the splinter of the amorphous region of cellulose was found during the structural investigation. In this investigation, it was assessed that thermal pre-treatment

affects porosity, grain size, and the propagation of cracks. It happened due to the violent escape of moisture from the surface of biomass. These structural defects mainly influence the heat transfer characteristic of biomass during pyrolytic reactions.

3.3. Thermal performance of pine needles in a small-scale reactor

The variation in the extensive property, mass, of pine needles pellets is shown in Fig.6. The initial mass of 300 g was chosen for experimental purpose. Each test was repeated thrice, and the average values were considered. It was noticed that the relative size of the mass plateau during dehydration was reduced by 56% for the pine pellets when it was compared with the wood chips. The formation of ripples was observed at the onset of pyrolysis. This ripple effect was formed either due to a surge in the heating rate of the system or the formation of intermediary compounds. As the applied voltage and power supply is constant, thermal lag was noticed during the thermal degradation of pine pellets. It implicated that thermal immunity of pre-treated biomass at a lower temperature range was slightly increased due to the cross-linking or carbonization reaction. The surface adsorption in processed pine needles pellets caused a temperature drop of 15 °C at the beginning of the char formation and corresponding to this change in temperature, the dynamic pressure of the system was reduced from 0.6 Pa to 0 Pa. It was deduced from the TG curves that surface cracking during thermal pre-treatment had changed the TG behaviour of the processed pine pellets.

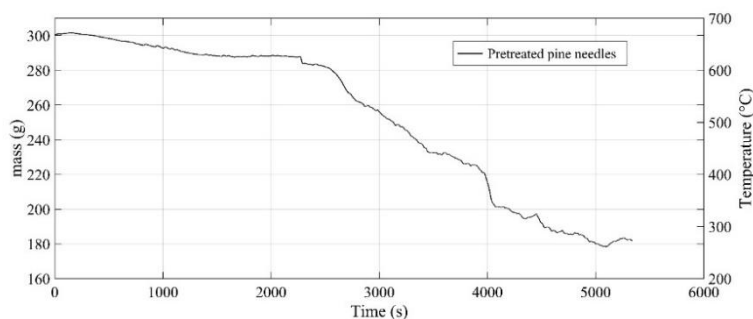


Fig. 6. Mass distribution of torrefied pine needles in a small-scale reactor

Apart from thermogravimetric variation in the mass of torrefied pine needles pellets, the intensive properties of the system, temperature and pressure were also got affected by the change in the course of thermal decomposition reactions. The change in the intensive properties of the fixed bed reactor is shown in Fig. 7. At the same electrical supply, a remarkable surge in the lower bed temperature (A) was noticed at the beginning of the thermal degradation of the pre-treated pine

pellets. The heating rate was estimated to be $3.89\text{ }^{\circ}\text{C}\cdot\text{min}^{-1}$ during this thermal event. The sigmoidal behaviour or undulation in thermal histories signified that the dissipation of heat and pressure was taken place simultaneously within the system. As the lower bed (A) reached the cut-off point, the upper bed temperature (B) attempted to attain thermal equilibrium with the thermal profile of the lower bed (A). It was noticed that the heating rate was increased by 24.26% as desorption in the torrefied pine pellets was taken place. The desorption of moisture was carried out at the heating rate of $6.76\text{ }^{\circ}\text{C}\cdot\text{min}^{-1}$. The drying or desorption of moisture accompanied a pressure rise by 76%, which showed that the removal of moisture content in the torrefied pine pellets drifted away from its thermal equilibrium. This was happened due to a rise in the partial vapour pressure of water content in the cellulose structure. The internal structural failure of pine needles pellets during torrefaction bolstered the pressure-driven flows across the reactor, and consequently, reduced the residence time of volatile in the reactor. The evolution of volatile was noticed to occur in a temperature interval of $406\text{--}577\text{ }^{\circ}\text{C}$ in the torrefied pine pellets. The charring process of pine needle pellets was noticed to take place in a temperature range of $577\text{--}690\text{ }^{\circ}\text{C}$. The pressure drops that occurred during char formation was estimated to be 212 Pa. After the power supply was interrupted, the thermal lag was noticed to be subdued with time.

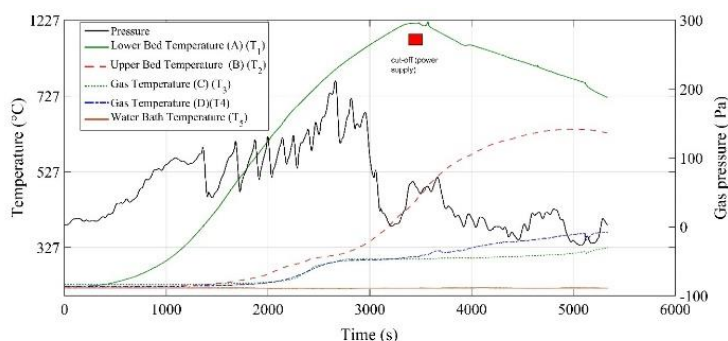


Fig. 7. Intensive (pressure and temperature) properties of a reactor

The producer gas composition derived from the thermal decomposition of the torrefied pine needles pellets is shown in Fig.8. It was noticed that the emission of CO_2 and CO fraction was reduced by 8.2% and 12% respectively. Likewise, the percentages of hydrogen and methane were found to increase by 91.2% and 11%, respectively. The net emission was cut by 20.2% after the pre-treatment of pine needles pellets when it was compared to the hardwood Chips. It was observed that the release of volatiles was very abrupt as time proceeds. It happened due to the reaction of carbon monoxide with the water vapour and ultimately, the

increase in hydrogen gas percentage was noticed. The carbon dioxide and methane gases were saturated as the hydrogen gas began to rise.

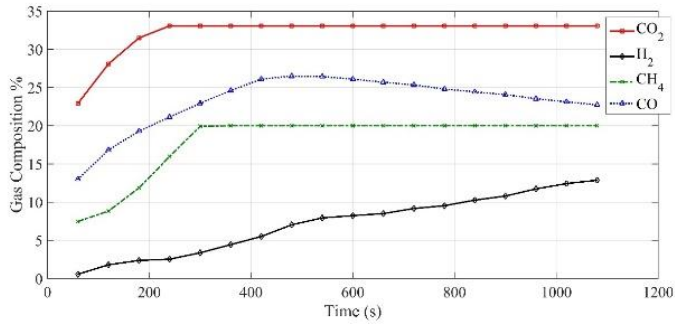


Fig. 8. Composition of producer gas derived from torrefied pine needles pellets

The thermal performance and miscellaneous parameters associated with the fixed-bed reactor is provided in Table 1. The consumption rate of the torrefied pine pellets was computed to $232 \text{ g}\cdot\text{h}^{-1}$, which was found to be 51% lower than that of Wood chips). On the other hand, the specific pyrolysis rate (SPR) of the pre-treated pine pellets was estimated to be $40590 \text{ g}\cdot\text{m}^{-2}\cdot\text{h}^{-1}$, which was reduced by 25% when it was compared with wood chips.

Table. 1. Thermal parameters related to thermal decomposition of processed pine needle pellets

Parameters	Values
FCR	$232 \text{ g}\cdot\text{h}^{-1}$
SPR	$40590 \text{ g}\cdot\text{m}^{-2}\cdot\text{h}^{-1}$
SGPR	$7.58 \text{ m}\cdot\text{h}^{-1}$
τ	3 h
η_t	85.42%
η_c	85.25%
η_h	86%
Char yield	60%
Oil yield	10.48%
Gas yield	12%
ω	$0.0155 \text{ kg w.v/kg d.a}$
γ	31.032%
ψ	4.73
$\left(\frac{\Delta P}{L}\right)_b$	$1.8 \text{ Pa}\cdot\text{m}^{-1}$

The drop in SPR was mainly happened due to the geometrical design of the reactor. Some other reason could to deviation in porosity of the pine pellets upon

thermal pre-treatment. As the volatile gases penetrate the carbon particle and lead to the displacement of carbon. Consequently, the resultant gas is allowed to diffuse through the solid structure and trigger pyrolysis reactions. During the release of volatile, some materials get swollen and become more porous. These activated porous sites allow the volatile gases to react with the carbon and form the byproducts of pyrolysis. These local porosity and permeability are also affected by the presence of surface cracks that eventually causes the change in pressure during oxidation, and thus the rate of reaction is impacted. The specific gas production (SGPR) was calculated to be $7.58 \text{ m}\cdot\text{h}^{-1}$, which is way too higher than that of wood chips. Owing to the volumetric flow of nitrogen, the decrease in the overall percentage of the producer gas composition was noticed during the pyrolysis of wood chips. Therefore, the nitrogen-based reactors are efficient enough for the gas production for the lower thermal history. The water vapour estimated to be 0.0155 kg per unit of dry gas.

3.4. Thermal performance of pine cones in a small-scale reactor

The variation in the extensive and intensive properties of the system during thermal decomposition in a fixed bed reactor is shown in Fig. 9. Similar to torrefied pine needles, 300 g of processed pine cones pellets were used to run the small-scale reactor at the bed temperature of 700°C . It was seen that the mass plateau formed during dehydration of water is reduced by 28% when it was compared with wood chips. Similarly, the devolatilization stage of processed pine cones was shrunk by 79% when it was compared with hardwood chips. The rate of conversion of processed pine cones at the starting of pyrolysis was reduced by 92.2%. Similar to the torrefied pine needles, thermal immunity in torrefied pine cones were also noticed. Unlike the raw pine cones, the torrefied pine cones were found to be slightly ruptured along their length during the morphological study, which made the heat transport more quickly inside the interior and influences the permeability of the volatile gases. Consequently, it allowed thermal energy to transfer through the char layer to the unreacted portion of the processed pine cones by the conduction, and thus promote the char formation reaction. The drying of processed pine cones was carried out in the temperature interval of $30\text{--}113.5^\circ\text{C}$ with a heating rate of $5^\circ\text{C}\cdot\text{min}^{-1}$, whereas the devolatilization of the processed pine cones occurred at $133.5\text{--}677^\circ\text{C}$. The formation of char was taken place at $627\text{--}693^\circ\text{C}$. The acceleratory phase accompanies the declaratory phase in the temperature profile was occurred due to a change in the pressure and heat of reaction during thermal decomposition of processed pine cones. Owing to condensation of volatile gases at macropores and dilation of grain size had

increased the secondary char during pyrolysis of the torrefied pine cones. This could be enhanced if the direction of heat flow with respect to grain orientation is changed.

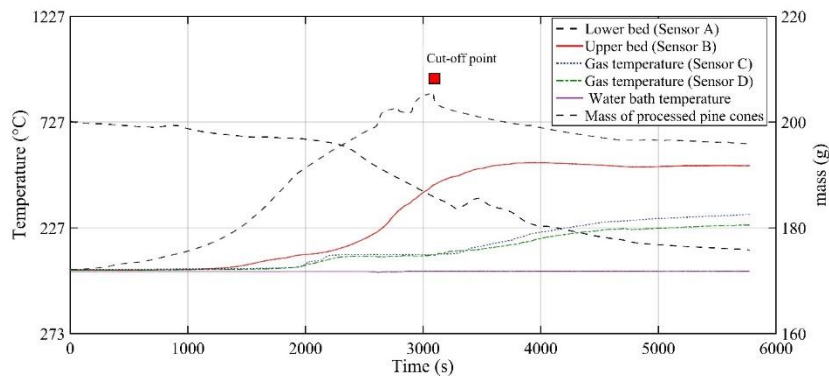


Fig. 9. The change in mass and temperature of torrefied pinecone pellets

The change in the pressure inside the fixed-bed reactor was shown in Fig. 10. The rate of change of dynamic pressure at the beginning of pyrolysis was estimated to vary from $0.06\text{--}0.07\text{ Pa}\cdot\text{s}^{-1}$. The pressure inside the reactor was reduced by 68% at the onset of char formation of processed pine cones. The peak pressure of 954 Pa was obtained at common boundaries of devolatilization and char formation regions. Besides the rapid fluctuation in the pressure of the system, the phenomenon of surface adsorption was seen at the junction of devolatilization and char formation regions.

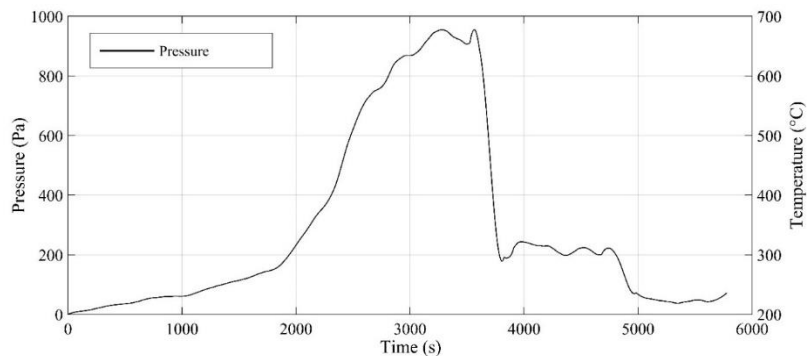


Fig. 4.17. Variation in the pressure of the producer gas generation during pyrolysis of torrefied pinecone pellets

A sharp drop of 5% was estimated for processed pine cones, which is further reduced by 55.34% as time proceeds. The pressure of volatile gases was found to be elevated by 4.2% once the surface adsorption was faded away with time.

The parameters related to the thermal performance of processed pine cones were tabulated in Table 2. The fuel consumption rate (FCR) of processed pine cones was computed to be 127 g-h^{-1} , which was found to be 73% lower than that of hardwood chips.

Table. 2. Thermal parameters related to thermal decomposition of processed pine cones pellets

Parameters	Values
FCR	127 g-h^{-1}
SPR	$22280 \text{ g-m}^{-2}\text{-h}^{-1}$
SGPR	28.19 m-h^{-1}
τ	9.8 h
η_t	90.40%
η_c	90.30%
η_h	90.60%
Char yield	48%
Oil yield	13%
Gas yield	36.54%
ω	0.011 kg (w.v)/kg (d.g)
γ	37.73%
ψ	0.98
$\left(\frac{\Delta P}{L}\right)_h$	5.30 Pa-m^{-1}

The char yield derived from processed pine cones was computed to be 48% for the given design of the reactor. A 78% rise in char production was recorded as compared to the wood chips, whereas the marginal rise of 1.5% over the hardwood chips was seen in the gas yield. The SPR for the given reactor when it was run by processed pine cones was calculated to be $22280 \text{ g-m}^{-2}\text{-h}^{-1}$. The reactor running in the presence of nitrogen gas has an SPR of $50000 \text{ g-m}^{-2}\text{-h}^{-1}$, which is relatively 124.41% higher than that of a reactor running in the presence of limited air. The main reason for the drastic variation is the design of the reactor and the effect of forced convection on thermal decomposition. In the same way, the specific gas production of the reactor with processed pine cones was calculated to be 28.19 m-h^{-1} . The pressure drop across the fixed bed was computed to be 5.30 Pa-m^{-1} . As compared to processed pine needles, the pressure drop across the processed pine cones was found to be 194% higher. The reason is the sphericity (ψ) of pine cones with respect to the processed pine needles pellets

was reduced by 79.28%. The thermal efficiency was found to be 5.83% higher than that of processed pine needle pellets. Correspondingly, the cold and hot gas efficiencies of the reactor were estimated to be increased by 6% and 5.3% respectively when it was powered by processed pine cones. Upon comparing it with wood chips, the cold gas efficiency of the reactor obtained from processed pine cones was surged by 14.30%, whereas the hot gas efficiency was increased by 6.58%. The gas composition obtained after thermal degradation of pine cones is shown in Fig. 11. The emission of CO₂ from the processed pine cones pellets was dropped by 20% when it was compared with woodchips, whereas the percentage of methane in the producer gas was computed to be 6.44% higher than that of wood chips.

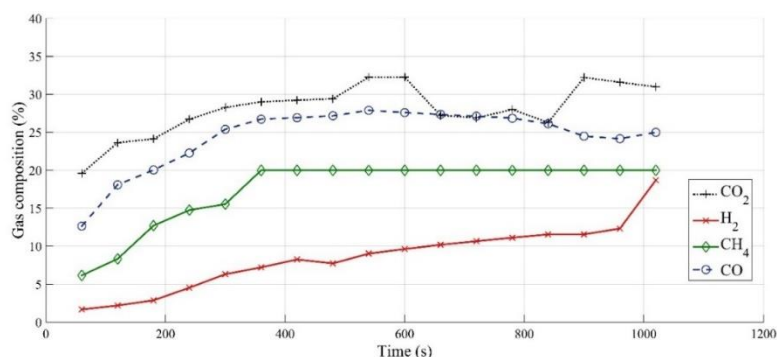


Fig. 11. Composition of producer gas derived from torrefied pinecone pellets

The emission of CO and CO₂ from thermally pretreated pine needles was relatively curtailed by 11.61% and 8.17%, respectively, as compared to emission generated by the wood pellets. Similarly, the two greenhouse gases (CO and CO₂) emission from thermally pretreated pine cones was reduced by 3.6% (CO₂) and 3.74% (CO) as compared to raw pine cones, whereas it was decreased by 20% (CO₂) and 6% (CO) with respect to the unprocessed wood pellets. The clean gas production by thermally processed pine cones to the commercial wood pellets (Hog fuel) was increased by 6.44%, whereas it was 10.49% in the case of thermally processed pine needles. Relatively speaking, the gas content derived from processed pine waste was much cleaner than that of the wood chips and wood pellets. As compared to processed pinecones, a 63% cleaner gas was derived from thermally pretreated pine needles.

3.5. Heat of reaction for pine needles

The distribution of heat of reaction among different regimes of pyrolysis at ramp rates of $5\text{ }^{\circ}\text{C}\cdot\text{min}^{-1}$ and $15\text{ }^{\circ}\text{C}\cdot\text{min}^{-1}$ was derived with the help of DTA curves, which are shown in Fig. 12 (a & b).

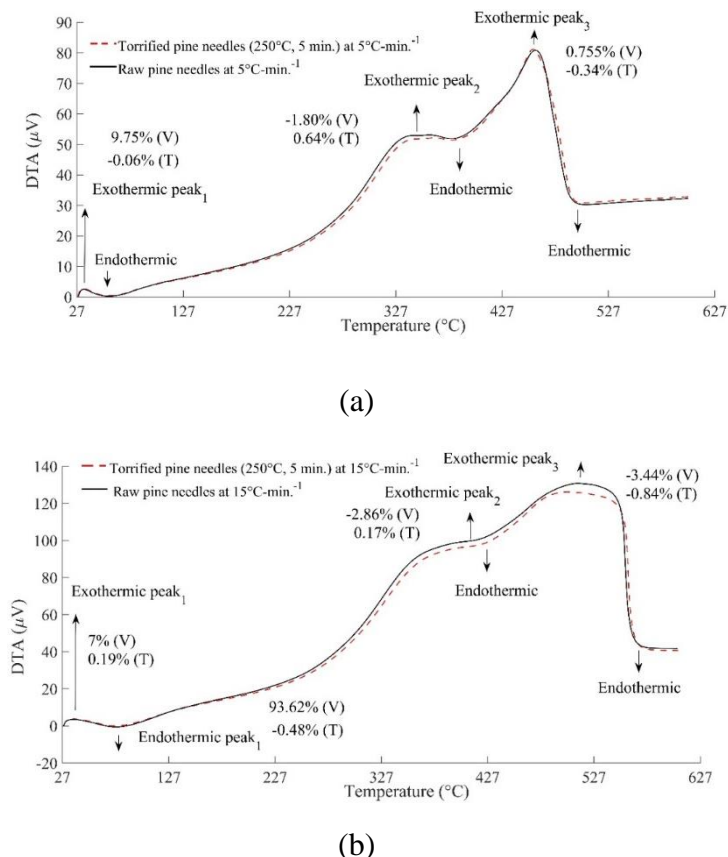


Fig. 12. The change in heat of reaction of pine needles at different heating rates (a: $5\text{ }^{\circ}\text{C}\cdot\text{min}^{-1}$, b: $15\text{ }^{\circ}\text{C}\cdot\text{min}^{-1}$)

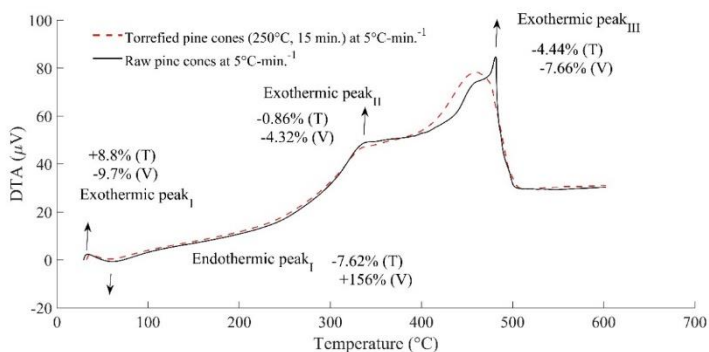
The upward arrows denote the exothermic reactions, whereas the downward direction shows the endothermic heat of the reaction. For the raw pine needles, the first exothermic region was noticed to be stretched from 28.2 $^{\circ}\text{C}$ to 33.2 $^{\circ}\text{C}$. Similarly, the second and third exothermic peaks were lying in the temperature interval of 250–336.3 $^{\circ}\text{C}$ and 337–601.89 $^{\circ}\text{C}$, respectively. Concerning raw pine needles, the exothermic heat of reactions (I) and (III) of torrefied pine needles were increased at a low heating rate, whereas the temperature range was noticed to be shifted in the left direction. On the other hand, the voltage gain at the second exothermic region was reduced. However, the overall rise in the heat of reaction was noticed for torrefied pine needles.

Likewise, the higher ramping rates characterised the peak regions of the torrefied pine needles by showing much more ripples in the magnitude of voltage and temperature than that of raw pine needles. Relatively speaking, the endothermic heat of reactions of the torrefied pine needles were seen to be decreased with increasing the heating rates and the magnitude of the exothermic heat of reaction were increased. The net energy loss during the pyrolysis process takes place to decompose the hydrolysed part of the raw material. The overall capital gain is estimated to vary from 0.1 ¢ to 0.29 ¢ per kg of pine needles if torrefied pine needles are used in place of raw pine needles. However, for both the materials, the drop in the heat of reaction (II) (Exothermic) was noticed at the heating rate of 15 °C-min⁻¹, whereas the region (III) of the torrefied pine needles were shrunk in magnitude, which made the overall heat of the system less exothermic than that of the raw pine needles at a heating rate of 5 °C-min⁻¹.

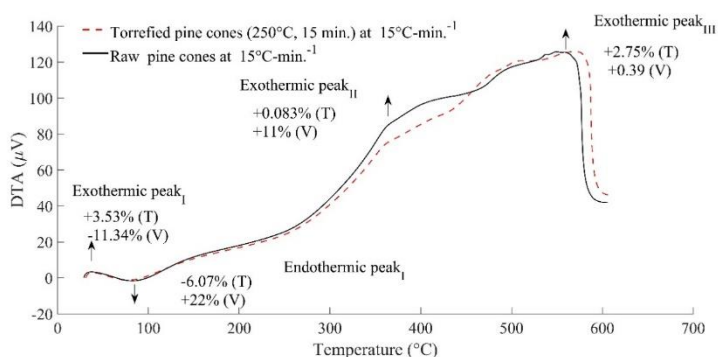
3.6. Heat of reaction for pine cones

Differential thermal analysis (DTA) of both the torrefied and raw pine cones at different ramp rates as illustrated in Fig. 13. The temperature range for the exothermic region (I) was estimated to be 8.8% higher than that of the exothermic region (I) of the raw pine cones. The voltage drop corresponding to the power of the system was computed to be 9.7% at the onset of pyrolysis. The range of temperature during dehydration of the torrefied pine cones was reduced, which implied that the corresponding heat of reaction (Endothermic) was also mitigated by 7.62% during dehydration of the torrefied pine cones. Similarly, the heat of reaction (Exothermic II) during the release of volatiles was also curtailed by 2.55% in the case of torrefied pine cones. A marginal change of around 0.15% between the heat of reactions of the raw and the torrefied pine cones was noticed as both the materials underwent the char formation at a heating rate of 5 °C-min⁻¹. Likewise, the deviation in the local maxima and minima over a given range of temperature was seen at higher ramping rates. The distribution of heat of reaction among different stages of pyrolysis was found to be disrupted due to the formation of the intermediate products, which resulted in the formation of an additional number of peaks in the given stage. This phenomenon was noticed at 15 °C-min⁻¹. These additional peaks encompassed 12% of the total heat of reaction whilst carrying out pyrolysis of raw pine cones at a higher ramping rate, whereas, in the case of torrefied pine cones, this share was augmented by 19.2% at the same heating rate. The relative variation of temperature range at Endothermic peak I was reduced by 30% as the heating rate increased from 5 °C-min⁻¹ to 15 °C-min⁻¹. Similarly, the temperature over which devolatilisation was taken place, was also

increased by 34.88–110% with the increase in the heating rate, which was estimated to be 84 to 162% during char formation. The energy released during the charring process to the ambience was found to be 50–52% lesser at $15^{\circ}\text{C}\cdot\text{min}^{-1}$ than that of $5^{\circ}\text{C}\cdot\text{min}^{-1}$. The overall heat of reaction was reduced 0.8–32% for the torrefied pine cones, whereas it was 0.6–41% for the raw pine cones. The conclusion can be drawn from this fact that the variation of the reaction heat in the torrefied is lower than that of its raw form. The energy burden on the system was increased at a higher ramping rate.



(a)



(b)

Fig. 13. The change in heat of reaction of pine cones at different heating rates (a: $5^{\circ}\text{C}\cdot\text{min}^{-1}$, b: $15^{\circ}\text{C}\cdot\text{min}^{-1}$)

4. NEW SCIENTIFIC RESULTS

The torrefaction process on the pine waste was exhaustively investigated and the various elements were highlighted in the different sub-heading. The following points were found to be noteworthy:

1. Physico-chemical analysis

According to physical and chemical evaluation, I observed that it was not necessary that the hydrogen and oxygen would simultaneously decrease with increasing torrefaction temperature. So far, it was reported in the literature that both hydrogen and oxygen would decrease, but to what extent a fall takes place. I evaluated that the higher thermal history would only allow the hydrogen molecules to disintegrate from the structure. In fact, on the contrary, in some cases, the overall hydrogen fraction would increase and only oxygen would be driven off the structure. I noticed that the different material would showcase anomaly in the elemental behaviour. I had investigated that the material with higher volatile content could not withstand a higher duration of processing and mass yield drop would be phenomenal. Comparatively, I noticed that pine cones would support temperature orientated torrefaction, whereas the leaf part, pine needles, would largely rely on torrefaction time. I ferreted out the fact that both time and temperature would govern the thermal event associated with the torrefaction process. The ash content would increase with increasing both time and temperature for pine cones. On the other hand, it would only decrease with increasing torrefaction temperature and reducing the processing period. The calorific value for pine needles would only be increased if torrefaction is conducted for a higher temperature regime, whilst it is governed by the processing period in pine cones.

2. Morphological investigation of pine waste

I noticed that the grain shifting, dilation of boundaries and the propagation of surface cracks were predominant on both pine needles and pine cones, which changed the heating characteristic of torrefied pine waste and influence the char yield upon pyrolysis. I found the dilation of grain boundary would increase the residence time of volatile gas and support the intermolecular condensation reaction that ultimately impacts the char formation reaction. With the change in the heating characteristic, the pressure-driven flow is reduced, and intra-particle residence time is increased, which finally encourage condensation reaction and char formation. To confirm this finding, I compared the results with G50 chips, and I noticed that the pressure was continuously rising from 10 Pa to 30 Pa during

the devolatilisation phase, whilst it was not true in the case of torrefied pine waste. It was decreased from 100 Pa to 0 Pa during the devolatilisation of torrefied pine waste. Thus, I confirmed that the condensation reaction would take a lead. The structural defect would bear upon the alternation in the reaction pathway.

3. Thermo-economic analysis of pine waste

I investigated that thermal decomposition of thermally pre-treated pine waste (unconventional biomass) mitigated emission of CO₂ by 8.17–20% and CO by 6–11.61% as compared to the commercial wood pellets (conventional biomass). Similarly, the clean energy production was increased by 6.44–10.49% after thermal pretreatment of pine waste. After the torrefaction process, I found that the loose biomass generated 63% much cleaner energy than the commercial wood pellets. I confirmed that the major emission reduction was during the water-gas shift reactions. I noticed the catalytic effect of flying ash, which ultimately bolstered the methanation of products of Water-gas shift reaction. I also found that the overall financial gain would be highest with those materials which have higher volatile content and the least processing cost. The percentage of CH₄ was significantly increased while carrying out the thermal decomposition of pre-treated pine cones and pine needles in a pilot-scale reactor. The drop in carbon emission and improvement in methane content showed that the torrefaction process provided a clean and less polluted source of energy. The torrefied pine needle pellets were seen to be lesser energy-intensive than that of torrefied pine cones. I estimated the relative financial incentive obtained from torrefied pine cones could be 81.83% lower than that of torrefied pine needles. Furthermore, I also observed that the processing of torrefied pine needles would be 30.20% lesser energy-intensive than that of torrefied pinecones. During the milling process, I noticed that the loose biomass, pine needles, would be 60% lesser energy-drain process than the solid biomass, pine cones. On the other hand, pelletisation of loose biomass would relatively require 35% less energy as compared to solid biomass. As compared to the commercial wood pellets, the electrical energy required by the pine waste was decreased by 11–21%. I estimated that the expected revenue generation from the pine waste char over the commercial biomass was \$0.31–1.37.

4. Thermochemistry of the torrefied pine waste

I validated via the microscopic analysis that the shift in energy balancing would be predominant, and I had noticed that the torrefied pine waste would be more exothermic in nature than its raw form. A torrefied material derived from a highly

volatile material, such as pine leaves, would have a higher heat of reaction if they are decomposed at a higher ramping rate, whilst the torrefaction of hard material, pine cones, would be more exothermic at a lower ramping rate than higher ramping rate. It happened due to a change in the grain orientation of pine waste upon torrefaction. I had seen that the lower heating rate in torrefied pine cones increased the residence time of volatile. Consequently, it triggered the autocatalytic reactions which are highly exothermic in nature.

5. Chemical kinetics of torrefied pine waste

I had seen that the multi-step reaction mechanism was followed by both the material. Pyrolysis of torrefied pine needles was shifted to higher-order diffusion-reaction along with nucleation and growth reaction regime. Unlike torrefied pine needles, torrefied pine cones were found to have more drastic variation in the reaction pathway. The higher-order power law, followed by higher orders of diffusion, nucleation and growth, and sigmoidal regimes would be the sequence of pyrolysis reaction in the torrefied pine cones. The nucleation was found to be more predominant in torrefied pine needles than that of torrefied pine cones, which eventually influenced the activation energies of the reaction.

5. CONCLUSION AND SUGGESTIONS

It was found that torrefied pine waste, pine cones and pine needles, had a severe impact on their physical, chemical and morphological characteristics. The time and temperature played a pivotal role to determine the calorific content of the torrefied pine waste. The torrefaction duration was found to have a phenomenal impact on the fixed carbon, volatile content, ash content and mass yield of torrefied pine needles, whereas temperature played a major role to decide the optimum energy yield. Alongside loose biomass, pine needles, a hard form of biomass was also torrefied. The torrefaction temperature was seen to have a hegemony over torrefaction duration when the constant sample of raw pine cones was thermally processed at 210–250 °C.

From the relative morphological study of pine needles, the longitudinal cracks of around 8.08–20.77 µm were formed after the torrefaction. The microfibrils were found to be disintegrated into small splinters. The pore size was dilated by 2.82–9.65 µm. The grain orientation was changed by 17° to 123°. The dilation of surface area was also noticed. Similarly, in torrefied pine cones, the holes of cellulose microfibrils of raw pine cones were stretched by 198.5%. The fissures of around 1.47–10.43 µm were formed between the grain boundaries of pine cones. The orientation of grain was deviated by 28–47°.

The emission of CO₂ from torrefied pine needles and pine cones pellets was estimated to be dropped by 20.2% and 20%, respectively, whereas methane was increased by 11% upon pyrolysis of torrefied pine needles. It was noticed that CO₂ and CO were saturated as the hydrogen gas was elevated. Similarly, the methane obtained from torrefied pine cones was reduced by 70% when it was compared with the torrefied pine needle pellets. The consumption rate of torrefied pine pellets was computed to be 232 g·h⁻¹, which was noticed to 83% higher than that of torrefied pine cones. The water generation per kg of the dry gas was found to be 41% higher with the torrefied pine needles pellets than that of the torrefied pine cones. The net exothermic heat of reaction for torrefied pine needles at a ramp rate of 5 °C·min⁻¹ was decreased by 43% when it was compared with torrefied pine cones, whereas a 14% rise in exothermic heat of reaction was recorded as the ramp rate was increased to 15 °C·min⁻¹. The net endothermic heat of reaction for the torrefied pine cones was reduced by 98% as compared to the torrefied pine cones at a heating rate of 5 °C·min⁻¹, whereas it was reduced by 97% for the torrefied pine needles with the increase in the heating rate to 15 °C·min⁻¹.

6. SUMMARY

PRE-TREATED PINE WASTE AS AN ALTERNATIVE ENERGY SOURCE

A comprehensive as well as qualitative analysis of one of biomass processing technologies, torrefaction, was carried out with the help of the quasi-static technique. Unlike the predominant studies carried out on the micro-wave oven, this work was performed on the joule heating system, where the existing furnace was improvised to serve the desired purpose. The objective of the study to determine the effect of operating condition on the torrefaction process. It was found in the study that the physical characteristic of biomass influenced the mass and energy yield of the torrefied materials. The material used in this study is different in physical structure. It was a combination of loose biomass and regular biomass. The effect of time and temperature on the elemental composition, molar ratio of H/C and O/C was found to be different. A breakthrough finding in the context of physiochemical analysis emphasises that it is not essential that hydrogen and oxygen would simultaneously decrease with a rise in processing temperature.

According to structural analysis, surface cracks, dilation of grain boundary, the change in grain orientation was taken place for both pine needles and pine cones. As a result of morphological distortion, the heating trait of the torrefied pine waste was also changed, which consequently, influenced the char formation. The dilation of grain boundary increased the residence time of volatile gas in a solid matrix and supported the intermolecular condensation reaction. Not only pathway of pyrolysis reaction was changed but also the pressure-driven flow was impaired. A pressure drop from 100 Pa to 0 Pa was noticed during devolatilisation. The emission of CO₂ and CO was reduced by 20%, whereas the percentage increase of 11% was estimated in Methane. The char yield obtained from torrefied pine needle pellet was found to be 60%, whereas it was 48% for the torrefied pine cones.

The effect of torrefaction on the heat fluxes of pine waste was also seen. The torrefied pine waste was found to be more exothermic in nature. However, the heat of the reaction was seen to be a function of the heating rate. The higher heating rate was seen to be favourable for the torrefied pine needles, whereas it was the lower ramp rate that enhanced the exothermic heat fluxes of the torrefied pine cones. The reason for the rise in heat fluxes was owing to a change in the grain orientation.

7. MOST IMPORTANT PUBLICATIONS RELATED TO THE THESIS

Refereed papers in foreign languages:

1. **Dhaundiyal, A.,** and Toth, L. (2021): Modelling of a torrefaction process using thermal model object, *Energies*, 14, 9, pp. 1-24. DOI:10.3390/en14092481 (IF: 2.702)
2. **Dhaundiyal, A.,** Bercesi, G., Atsu, D., and Toth, L.(2021): Development of a small-scale reactor for upgraded biofuel pellet, *Renewable Energy*, 170, pp.1197–1214. DOI:10.1016/j.renene.2021.02.057 (IF:7.387)
3. **Dhaundiyal, A.,** and Atsu, D. (2020): Exergy analysis of a pilot-scale reactor using wood chips. *Journal of Cleaner Production*, 279, pp. 1-11. DOI: 10.1016/j.jclepro.2020.123511 (IF:8.41)
4. **Dhaundiyal, A.,** Atsu, D. and Toth, L. (2020): Physico-chemical assessment of torrefied Eurasian pinecones. *Biotechnology for Biofuels* 13, 199, pp.1–20. DOI: 10.1186/s13068-020-01840-7 (IF:5.47)
5. **Dhaundiyal, A.,** Singh, S. B., Atsu, D., and Toth, L. (2020): Comprehensive analysis of pre-treated Austrian pine. *Fuel*, 287, pp. 1–13. DOI: 10.1016/j.fuel.2020.119605 (IF:6.593)
6. **Dhaundiyal, A.,** Toth, L., Bacskai, I., and Atsu, D. (2020): Analysis of pyrolysis reactor for hardwood (Acacia) chips, *Renewable Energy*, 147, pp.1979–1989. DOI: 10.1016/j.renene.2019.09.095 (IF:7.387)

International conference proceedings:

1. **Dhaundiyal, A., & Toth, L.** (2019): Calculation of kinetic parameters of thermal decomposition of forest waste using the Monte Carlo technique. *Environmental and Climate Technologies*, 24(1), 162–170. DOI: 10.2478/rtuect-2020-0010 Conference of Environmental and Climate Technologies (CONNECT), Riga, Latvia (Held at Riga Technical University in May 2019).
2. **Dhaundiyal, A., & Toth, L.** (2021): Thermal Modelling of Torrefaction Process Using Finite Element Method The 3R International Scientific Conference on Material Cycles and Waste Management (3RINCs), (Held at National Institute for Environmental Studies, Tsukuba, Japan in March 2021).